

Topological horseshoe analysis and field-programmable gate array implementation of a fractional-order four-wing chaotic attractor

En-Zeng Dong(董恩增), Zhen Wang(王震), Xiao Yu(于晓), Zeng-Qiang Chen(陈增强), Zeng-Hui Wang(王增会)
Citation: Chin. Phys. B . 2018, 27(1): 010503. **doi:** 10.1088/1674-1056/27/1/010503

Journal homepage: http://cpb.iphy.ac.cn; http://iopscience.iop.org/cpb

What follows is a list of articles you may be interested in

Parameter analysis of chaotic superlattice true random number source

Yan-Fei Liu(刘延飞), Dong-Dong Yang(杨东东), Hao Zheng(郑浩), Li-Xin Wang(汪立新)
Chin. Phys. B . 2017, 26(12): 120502. **doi:** 10.1088/1674-1056/26/12/120502

A hybrid strategy to control uncertain nonlinear chaotic system

Yongbo Sui(隋永波), Yigang He(何怡刚), Wenxin Yu(于文新), Yan Li(李燕)
Chin. Phys. B . 2017, 26(10): 100503. **doi:** 10.1088/1674-1056/26/10/100503

Identifying the closeness of eigenstates in quantum many-body systems

Hai-bin Li(李海彬), Yang Yang(杨扬), Pei Wang(王沛), Xiao-guang Wang(王晓光)
Chin. Phys. B . 2017, 26(8): 080502. **doi:** 10.1088/1674-1056/26/8/080502

Homoclinic and heteroclinic chaos in nonlinear systems driven by trichotomous noise

You-Ming Lei(雷佑铭), Hong-Xia Zhang(张红霞)
Chin. Phys. B . 2017, 26(3): 030502. **doi:** 10.1088/1674-1056/26/3/030502

Period-control and chaos-anti-control of a semiconductor laser using the twisted fiber

Sen-Lin Yan(颜森林)
Chin. Phys. B . 2016, 25(9): 090504. **doi:** 10.1088/1674-1056/25/9/090504

Topological horseshoe analysis and field-programmable gate array implementation of a fractional-order four-wing chaotic attractor*

En-Zeng Dong(董恩增)[1,†], Zhen Wang(王震)[1], Xiao Yu(于晓)[1], Zeng-Qiang Chen(陈增强)[2], and Zeng-Hui Wang(王增会)[3]

[1] *Tianjin Key Laboratory For Control Theory & Applications in Complicated Systems, Tianjin University of Technology, Tianjin* 300384, *China*
[2] *Department of Automation, Nankai University, Tianjin* 300071, *China*
[3] *Department of Electrical and Mining Engineering, University of South Africa, Florida* 1710, *South Africa*

(Received 20 September 2017; revised manuscript received 16 October 2017; published online 22 December 2017)

We present a fractional-order three-dimensional chaotic system, which can generate four-wing chaotic attractor. Dynamics of the fractional-order system is investigated by numerical simulations. To rigorously verify the chaos properties of this system, the existence of horseshoe in the four-wing attractor is presented. Firstly, a Poincaré section is selected properly, and a first-return Poincaré map is established. Then, a one-dimensional tensile horseshoe is discovered, which verifies the chaos existence of the system in mathematical view. Finally, the fractional-order chaotic attractor is implemented physically with a field-programmable gate array (FPGA) chip, which is useful in further engineering applications of information encryption and secure communications.

Keywords: fractional-order chaotic system, Poincaré map, topological horseshoe, field-programmable gate array (FPGA)

PACS: 05.45.–a, 05.45.Gg, 05.45.Pq **DOI:** 10.1088/1674-1056/27/1/010503

1. Introduction

At the beginning of 1960s, Lorenz published an essay in the study of atmospheric turbulence phenomenon,[1] which opened the prelude to the study of chaos phenomenon. In the following decades, more and more attention has been paid to the research and application of chaos. Some chaotic attractors have been proposed, such as Chua circuits,[2] Chen system,[3] Qi system,[4] etc. In recent years, with the development of fractional calculus, the fractional order chaotic system and its synchronization and control have aroused extensive interest and done in-depth researches,[5–10] for the fractional order system is a more generalized system than the integer order system.

So far, there is no strict definition of chaos, so it has become a hot topic to prove the existence of chaos by different methods. The chaotic dynamics can only be proved by using numerical analysis methods, such as the Lyapunov exponents, phase portraits, and Poincaré maps, this cannot be looked as the evidence for chaotic dynamics. It is necessary to theoretically investigate the chaotic characteristics of the systems. Combined with computer numerical method, the topological horseshoe theory can be easily used to prove the existence of chaotic attractors mathematically.[11–13]

Due to the high logic density, versatility and other features, the field-programmable gate array (FPGA) chip has been widely used in communication and signal processing. Currently, the FPGA implementation for integer order chaotic systems has obtained some achievements.[14,15] Because fractional order dynamical systems can more objectively reveal and describe the essential phenomena in nature than the system of integer order dynamics,[16] the physical realization of fractional order system has more important application value.[17]

From two aspects of theory and physical realization, the chaos existence of a fractional order system is studied comprehensively in this paper. First, we focus on verifying the chaotic dynamics of a fractional-order system based on the topology horseshoe theory, the chaotic existence of the fractional order system is strictly proved mathematically. Furthermore, for the convenience of chaotic engineering applications, a digital circuit is designed to realize the fractional-order system based on the FPGA chip, which verifies the chaotic characteristics physically, and provides a general method of realizing chaos by FPGA.

In this paper, the fractional order four-wing system is investigated. The rest of the paper is arranged as follows. In Section 2, the fractional order four-wing system is constructed, and some phase portraits, Lyapunov exponent diagrams, and bifurcation diagrams are given to show its complex dynamic characteristics. Then, in Section 3, some topological horseshoe theory is reviewed firstly, and the existence of chaos is rigorously verified based on the topological horseshoe theory. In Section 4, the fractional order chaotic system is physically

*Project supported by the National Natural Science Foundation of China (Grant Nos. 61502340 and 61374169), the Application Base and Frontier Technology Research Project of Tianjin, China (Grant No. 15JCYBJC51800), and the South African National Research Foundation Incentive Grants (Grant No. 81705).

†Corresponding author. E-mail: dongenzeng@163.com

© 2018 Chinese Physical Society and IOP Publishing Ltd

implemented by using FPGA chip, the experiment results are consistent with the numerical simulations.

2. Fractional-order four-wing attractor

Dong et al. proposed an integer order four-wing chaotic attractor,[18] whose chaotic properties were verified by using the topological horseshoe and numerical calculations.[14] To obtain a more generalized system, a corresponding fractional order system is constructed as follows:

$$\begin{cases} \dfrac{\mathrm{d}^{\alpha}x}{\mathrm{d}t^{\alpha}} = ax - byz, \\ \dfrac{\mathrm{d}^{\beta}y}{\mathrm{d}t^{\beta}} = -cy + xz, \\ \dfrac{\mathrm{d}^{\gamma}z}{\mathrm{d}t^{\gamma}} = kx - dz + xy, \end{cases} \tag{1}$$

where a, b, c, $d \in R$, $0 < \alpha$, β, $\gamma < 1$, and parameters α, β, and γ are called fractional order.

The fractional derivative adopted in this study is the well-known Riemann–Liouville definition

$$\frac{\mathrm{d}^{q}f(t)}{\mathrm{d}t^{q}} = \frac{1}{\Gamma(n-a)}\frac{\mathrm{d}^{n}}{\mathrm{d}t^{n}}\int_{0}^{t}\frac{f(\tau)}{(t-\tau)^{q-n+1}}\mathrm{d}\tau. \tag{2}$$

This is because the fractional differential calculation of the system is difficult to calculate in the time domain and there is direct relationship of Laplace transform. In this paper, the frequency-domain approximation method will be used to analyze the fractional-order four-wing system, which has also been adopted in some other papers.[19–24]

In this study, all the initial values of system (1) are set to be zero, and the Laplace transform of the Riemann–Liouville definition is

$$L\left\{\frac{\mathrm{d}^{q}f(t)}{\mathrm{d}t^{q}}\right\} = s^{q}L\{f(t)\}. \tag{3}$$

The Laplace transformation of the system (1) is

$$\begin{cases} s^{\alpha}\boldsymbol{X}(s) = a\boldsymbol{X}(s) - b\boldsymbol{U}(s), \\ s^{\beta}\boldsymbol{Y}(s) = -c\boldsymbol{Y}(s) + \boldsymbol{V}(s), \\ s^{\gamma}\boldsymbol{Z}(s) = k\boldsymbol{X}(s) - d\boldsymbol{Z}(s) + \boldsymbol{W}(s). \end{cases} \tag{4}$$

$$\begin{aligned} \boldsymbol{U}(s) &= \boldsymbol{L}[u(t)] = \boldsymbol{L}[y(t)z(t)], \\ \boldsymbol{V}(s) &= \boldsymbol{L}[v(t)] = \boldsymbol{L}[x(t)z(t)], \\ \boldsymbol{W}(s) &= \boldsymbol{L}[w(t)] = \boldsymbol{L}[x(t)y(t)]. \end{aligned}$$

Based on the Porter frequency domain approximation method,[25] the approximation of the transfer function $1/s^{q}$ in the frequency domain is

$$\frac{1}{s^{0.9}} = \frac{2.2675(s+1.292)(s+215.4)}{(s+0.01292)(s+2.154)(s+359.4)}. \tag{5}$$

In this study, the fractional orders are set to be the same value which means $\alpha = \beta = \gamma$. With (a) constants $b = 1$, $c = 10$, $d = 4$, $k = 1$, $\alpha = \beta = \gamma = 0.9$, and varying a, (b) constants $a = 4$, $c = 10$, $d = 4$, $k = 1$, $\alpha = \beta = \gamma = 0.9$, and varying b, (c) constants $a = 4$, $b = 1$, $d = 4$, $k = 1$, $\alpha = \beta = \gamma = 0.9$, and varying c, (d) constants $a = 4$, $b = 1$, $c = 10$, $k = 1$, $\alpha = \beta = \gamma = 0.9$, and varying d, the four bifurcation diagrams of the variable x in the fractional order are shown in Fig. 1, which indicates that the chaos behavior exits in the fractional-order system when any of system parameters varies.

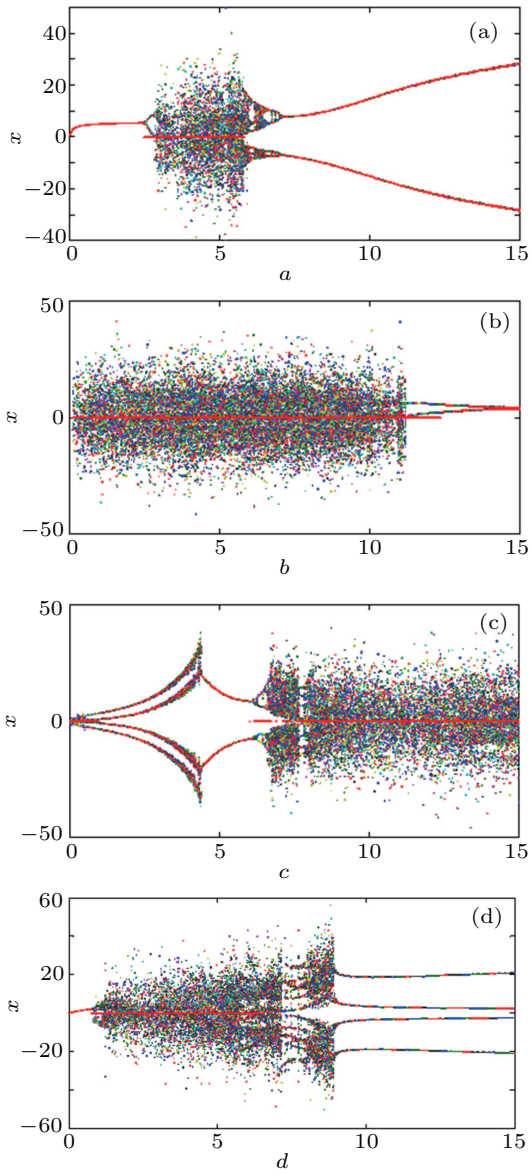


Fig. 1. (color online) Bifurcation diagrams for the 2.7 order fractional four-wing system, with (a) varying a, (b) varying b, (c) varying c, and (d) varying d.

Phase portraits can explicitly show the chaotic attractors. The phase portraits of this fractional order system are shown in Fig. 2. As can be seen from Fig. 2, the fractional-order system displays a four-wing chaotic attractor when selecting parameters are $a = 4$, $b = 1$, $c = 10$, $d = 4$, $k = 1$.

The Lyapunov exponent spectrum is given in Fig. 3 which can show its complex chaotic dynamics.

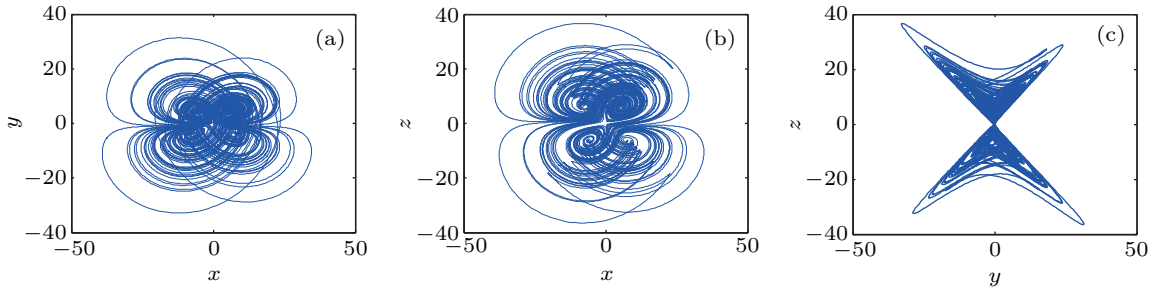


Fig. 2. (color online) Phase portraits of the 2.7 order fractional four-wing chaotic attractor (a) projection on x–y plane; (b) projection on x–z plane; (c) projection on y–z plane.

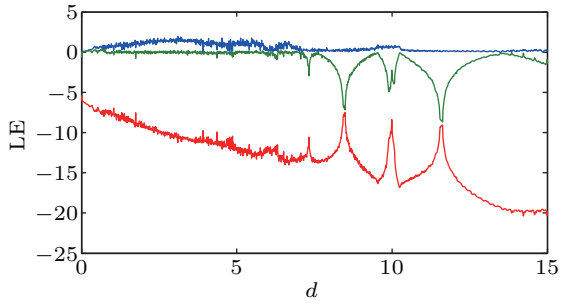


Fig. 3. (color online) Lyapunov exponent diagram (varying d).

3. Topological horseshoe analysis and verification

3.1. Review of topological horseshoe theory

The topological horseshoe theory can trace back to the well-known Smale horseshoe map proposed by Smale,[26] and it was expanded by Kennedy *et al.*,[27] Kennedy and York.[28] On the basis of the above researches, Yang *et al.*,[29] Yang and Li[30,31] proposed the topological hoof theory, which provides a computer aided method for theoretically proving whether a system is chaotic.[29–31]

Firstly some aspects of symbolic dynamics are recalled. Let $S = \{0,1,\ldots,N\}$, $N \geq 2$ be the set of non-negative successive integers. Let Σ be the collection of all bi-infinite sequences with their elements of S, i.e., each element s of Σ implies $s = \{\ldots,s_{-n},\ldots,s_{-1},s_0,s_1,\ldots,s_n,\ldots\}$, $s_i \in S$. Now consider another sequence $\bar{s} \in \Sigma$, $\bar{s} = \{\ldots,\bar{s}_{-n},\ldots,\bar{s}_{-1},\bar{s}_0,\bar{s}_1,\ldots,\bar{s}_n,\ldots\}$, $\bar{s}_i \in S$, the distance between s and $\bar{s}$ is defined as

$$d(s,\bar{s}) = \sum_{-\infty}^{\infty} \frac{1}{2^i} \frac{|s_i - \bar{s}_i|}{1+|s_i-\bar{s}_i|}. \tag{6}$$

With the distance defined as expression (6), Σ is a metric space, and there is a well-known theorem.

Lemma 1[29,32] The space Σ is (i) compact; (ii) totally disconnected; (iii) perfect.

A set having the three properties in the above theorem is generally referred to as a Contor set, which frequently appears in the characterization of complex structures of an invariant set in a chaotic dynamical system. Furthermore, consider a map of Σ into itself, $\sigma : \Sigma \to \Sigma$, given by

$$\sigma(s_i) = s_i + 1. \tag{7}$$

which is referred to as the m-shift map, and thus there is the following fact.

Lemma 2[33,34] (a) $\sigma(\Sigma) = \Sigma$ and σ is continuous; (b) the shift map σ as a dynamical system defined on Σ has the following properties:

i) σ has a countable infinity of periodic orbits consisting of orbits of all periods;

ii) σ has an uncountable infinity of nonperiodic orbits;

iii) σ has a dense orbit.

Thus, the dynamics generated by the shift map σ displays sensitive dependence on initial conditions on a closed invariant set, and therefore is chaotic.

Let X be a metric space, then Q will be a compact subset of X, and $f : Q \to X$ will be a map satisfying that $Q_1, Q_2, \ldots, Q_m$ are m mutually disjoint compact subsets of Q, and $f|Q_i$ is continuous for each Q_i.

Definition 1 Let Γ be a compact subset of Q, if $\Gamma_i = \Gamma \cap Q_i$ $(i = 1,2,\ldots,m)$ is nonempty and compact, then Γ is called a connection with $Q_1, Q_2, \ldots, Q_m$. F is said to be an f-connected family, if F is a family of connections with $Q_1, Q_2, \ldots, Q_m$ satisfying the following property: $\Gamma \in F \Rightarrow f(\Gamma_i) \in F$.

Lemma 3[30,35] Suppose that there exists an f-connected family with $Q_1, Q_2, \ldots, Q_m$. Then there exists a compact invariant set $k \subset Q$, such that $f|Q_i$ is semi-conjugate to m-shift.

Lemma 4[31,36] There are two dynamical systems, i.e., compact metric spaces (X,f) and (Y,g). If (X,f) is semi-conjugate to (Y,g), then the topological entropy of f is not less than that of g, that is, $\mathrm{ent}(f) \geq \mathrm{ent}(g)$. If g is an m-shift map, then $\mathrm{ent}(f) \geq \mathrm{ent}(g) = \ln m$. When $m > 1$, it can be proved that the dynamical system is chaotic.

3.2. Horseshoe in the fractional-order four-wing system

To mathematically prove the existence of chaos by using topological horseshoe theory, an appropriate Poincaré section is constructed on plane $\Pi = \{(x,y,z) \in R^3 : x = 0\}$ firstly. As

shown in Fig. 4, the four wings of the attractor are patches of dense points, and the most representative four-wing orbit behavior of the chaotic attractor is revealed.

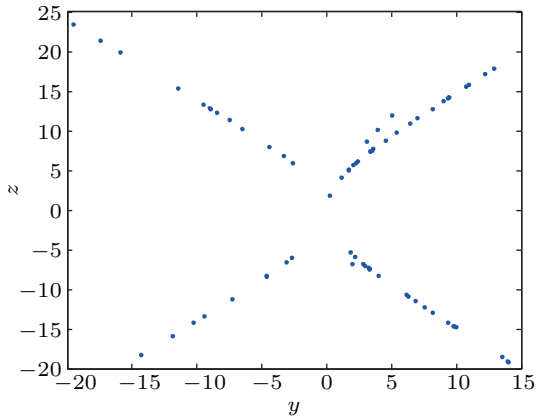


Fig. 4. (color online) Poincaré section of the attractor.

To construct a Poincaré map, a cross section X is selected on the plane Π, which intersects the one wing of attractor orbits. As shown in Fig. 5, $X = |MNPQ|$ with its four vertices $M = [0,0,0]$, $N = [0,0,30]$, $P = [0,25,30]$, $Q = [0,25,0]$.

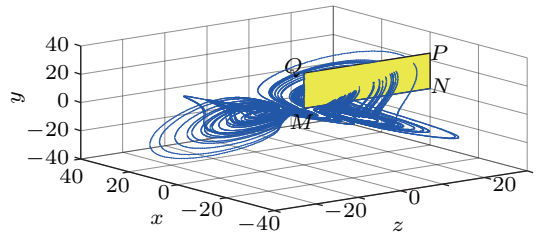


Fig. 5. (color online) Three-dimensional phase portraits and the selected cross section $X = |MNPQ|$.

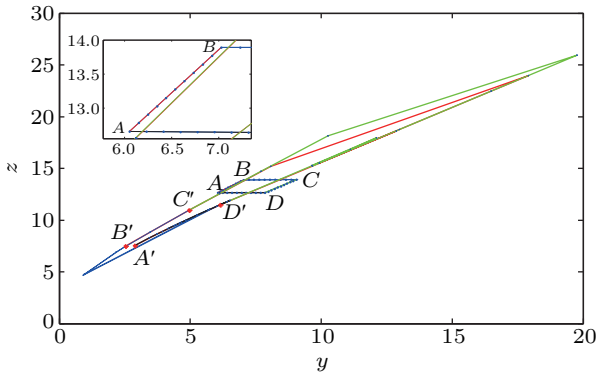


Fig. 6. (color online) Images $|A'B'C'D'|$ of the quadrangle $|ABCD|$, partially enlarged view in the inset.

Second, we need to seek a set U and its two mutually disjoint compact subsets in the cross section X, and define the corresponding first return Poincaré map $\omega : P \to \Gamma$ such that the image $\omega(P)$ intersects with the set P. After many tests and numerical calculations, the quadrangle $P = |ABCD|$ is selected to have four vertices $A = [0,6.05,12.66]$, $B = [0,7.027,13.895]$, $C = [0,9.05,13.925]$, $D = [0,7.859,12.635]$. As shown in Fig. 6, the image of $|ABCD|$ is like a very thin hook that wholly acrosses the quadrangle regions of $|ABCD|$.

The two mutually disjoint compact subsets are also found as shown in Fig. 7. Subset $|AGHD|$ has four vertices:

$$A = [0,6.05,12.66], \quad G = [0,6.655,13.424],$$
$$H = [0,8.566,13.401], \quad D = [0,7.859,12.635],$$

and subsect $|EBCF|$ has four vertices:

$$E = [0,6.664,13.432], \quad B = [0,7.027,13.895],$$
$$C = [0,9.05,13.925], \quad F = [0,8.578,13.412].$$

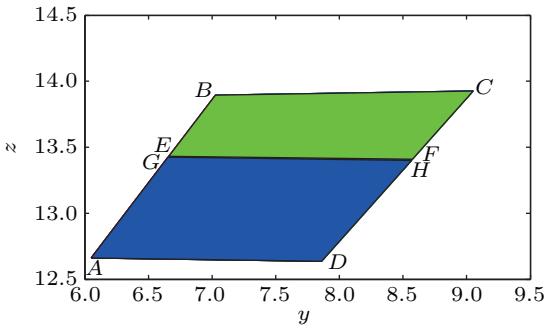


Fig. 7. (color online) Two mutually disjointed subsets $|AGHD|$ and $|EBCF|$.

Then, for the first return, the Poincaré map $\omega : P \to \Gamma$, $|E'B'C'F'| = \omega(|EBCF|)$, the image $|E'B'C'F'|$ is a very thin hook-like strip with BC mapped to $B'C'$ and EF mapped to $E'F'$. Furthermore, by enlarging the local region in Fig. 8, we can find that $E'B'$ and $C'F'$ are wholly situated across the set $|ABCD|$.

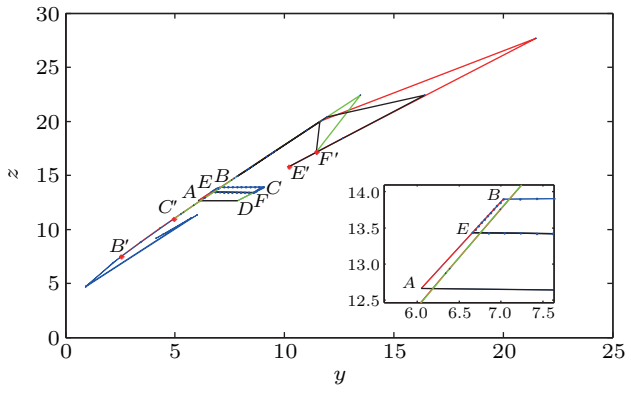


Fig. 8. (color online) Image $|E'B'C'F'|$ of the quadrangle $|EBCF|$, partially enlarged view is shown in inset.

The image of $|A'G'H'D'| = \omega(|AGHD|)$ is shown in Fig. 9, and AD and GH are mapped to $A'D'$ and $G'H'$, respectively. Similarly, $A'G'$ and $H'D'$ are wholly situated across the set $|ABCD|$.

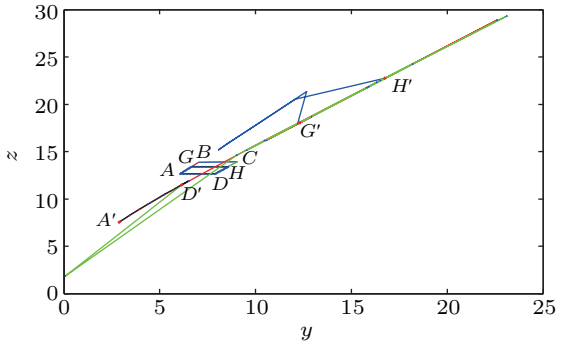


Fig. 9. (color online) Image $|A'G'H'D'|$ of the quadrangle $|AGHD|$.

Based on the above analysis, for each connection δ between the subset $|AGHD|$ and the subset $|EBCF|$ in set P, the images $\omega(\delta \cap AGHD)$ and $\omega(\delta \cap |EBCF|)$ also wholly cross the set P. That is, the images $\omega(\delta \cap AGHD)$ and $\omega(\delta \cap |EBCF|)$ are still connected between the subset $|AGHD|$ and the subset $|EBCF|$ in set P. According to Theorem 3 and Theorem 4, the map ω is semi-conjugate to the two-shift map, which shows that the entropy of the fractional-order four-wing system is $\text{ent}(f) \geq \log 2 > 0$. Thus, the presence of chaos in system (1) is proven.

4. FPGA implementation

FPGA is one of the highest integration degrees of application specific integrated circuit (ASIC), which solves the shortcomings of not only the custom circuit, but also the limited number of the gate circuits of the original programmable device. It has been used widely in modern digital signal processing due to its advantages, including internal programs running in parallel, a large number of soft cores and short development cycle.[37–39] As the chaotic signal can be used as an encrypted signal for secret communication, to better apply chaos to the communication area, the FPGA chip can be used to realize and validate the fractional order chaotic system.

For the convenience of engineering application, a digital chaotic circuit is designed and implemented by using an FPGA chip in this section.

As the FPGA is a digital device, it is necessary to discretize the chaotic system. In this paper, the transfer function is discretized by impulse invariance method[40]

$$H(S) = \frac{1}{S} \Rightarrow H(Z) = 0.001\frac{Z}{Z-1}. \tag{8}$$

The transfer function after discretization is as follows:

$$\begin{aligned} H(S) &= \frac{1}{s^{0.9}} \\ &= 0.001\frac{0.1126Z^3 - 0.1102Z^2 - 0.1126Z + 0.1102}{Z^3 - 2.964Z^2 + 2.929Z - 0.9645}. \end{aligned} \tag{9}$$

Based on the Blockset in the DSP Builder library, the model of Eq. (9) is built as shown below.

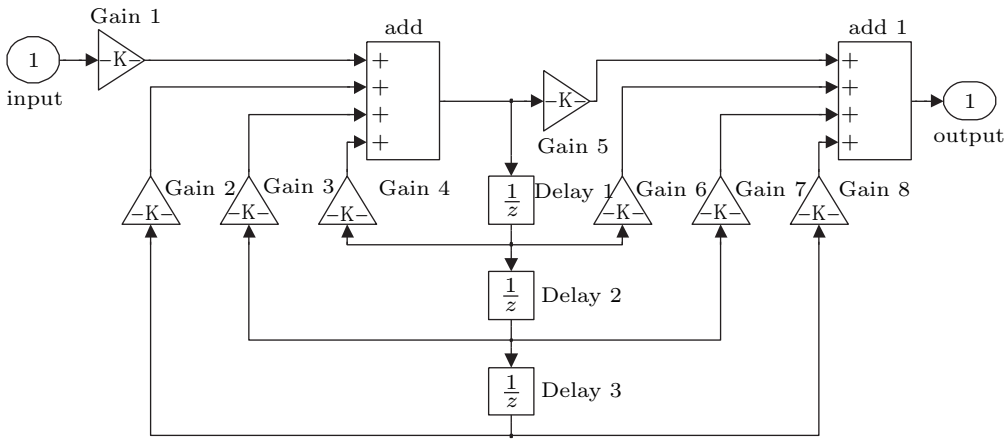


Fig. 10. Structure block diagram of $1/s^{0.9}$ after being discretized.

Here Gain 1 = 0.001, Gain 2 = 0.9645, Gain 3 = −2.929, Gain 4 = 2.2964, Gain 5 = 0.1126, Gain 6 = −0.1102, Gain 7 = −0.1126, Gain 8 = 0.1102. Add is an adder with four inputs, and Delay is a time delay device with a unit time delay.

As shown in Fig. 11, the structure model of system (1) is built by the DSP Builder Module.

After a successful simulation, the model file is converted into VHDL codes and the codes are analyzed, simulated, and compiled by using Quartus II. Finally the fractional-order chaotic system is implemented in the Alter DE2-115 development platform.

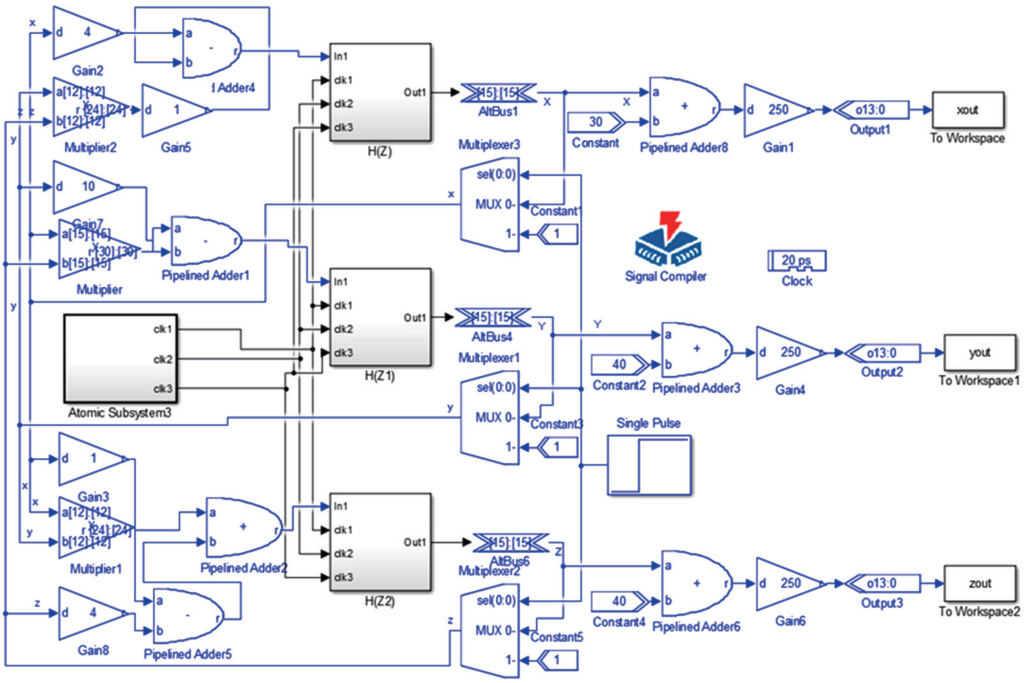


Fig. 11. (color online) Model structure of the fractional order four-wing system.

To facilitate the observing of the chaos attractor, in the experiment used is an AD9764 high-speed digital-analog conversion chip of 14 bits to convert the output digital signals of FPGA into analog signals. The clock frequencies of the D/A chip and the FPGA chip are synchronized at 50 MHz. Figure 12 shows the schematic of the experiment setup. The chaotic attractors generated by the FPGA are illustrated in Fig. 13.

The experimental results show that the chaotic attractors generated by the FPGA are consistent with the numerical simulations. This method is more convenient to apply to other chaotic system, providing further technical support for the application of a fractional chaotic system to the information encryption and secure communication.

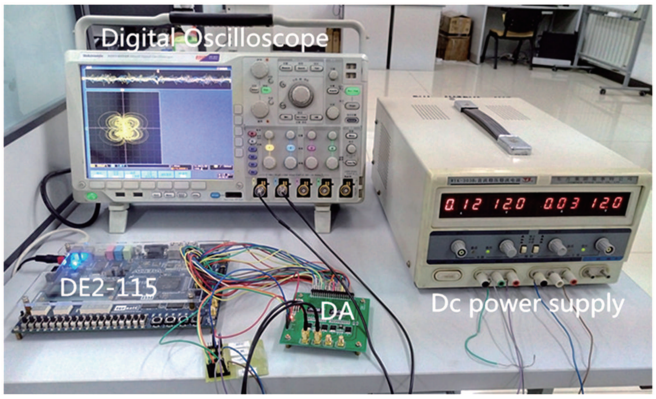


Fig. 12. (color online) Experiment setup.

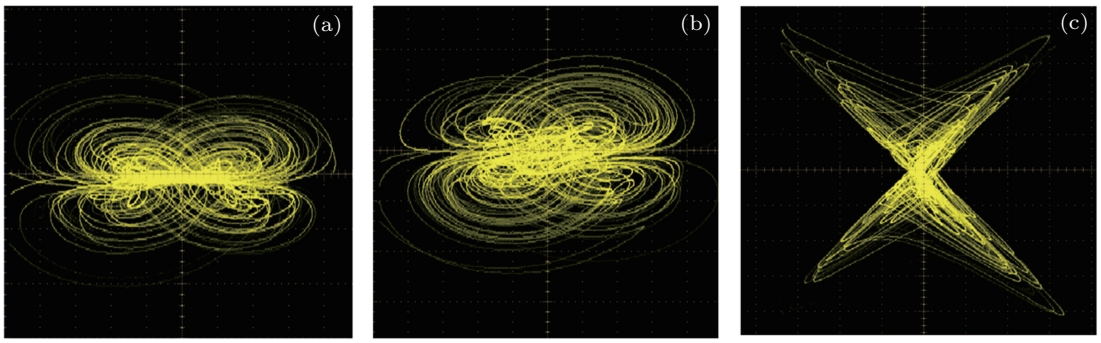


Fig. 13. (color online) Chaotic attractors generated by the FPGA, (a) projection on x–y plane, (b) projection on x–z plane, (c) projection on y–z plane.

5. Conclusions

In this paper, a fractional-order four-wing chaotic system is investigated. The Lyapunov exponent diagrams and bifurcation diagrams are used to verify the chaotic dynamics of the fractional-order system. Furthermore, based on the topology horseshoe theory, a suitable Poincaré section is selected

to obtain the corresponding Poincaré map, then, the horseshoe embedded in the attractor is found, which indicates that the system has positive topological entropy, and chaos is verified rigorously. Finally, a digital circuit is designed to realize the fractional-order system with the FPGA chip, and the chaotic characteristics are verified physically. All these research results show that the dynamics of the fractional-order four-wing system is complex. In the future we will apply this fractional system to information encryption.

References

[1] Lorenz E N 1963 *J. Atmos. Sci.* **20** 130
[2] Chua LO, Komuro M and T Matsumoto 1986 *IEEE Trans. Circuit Syst.* **33** 1072
[3] Chen G R and Ueta T 1999 *Int. J. Bifur. Chaos* **09** 1465
[4] Qi G Y, van Wyk B J, van Wyk M A and Chen G R 2009 *Chaos Soliton. Fract.* **40** 2016
[5] Danca M F and Tang W K S 2016 *Chin. Phys. B* **25** 010505
[6] Chen L P, Chai Y, Wu R W, Sun J and Ma T D 2012 *Phys. Lett. A* **376** 2381
[7] Liu H, Li S G, Sun Y G and Wang H X 2015 *Chin. Phys. B* **24** 090505
[8] Wang Q, Ding D S and Qi D L 2015 *Chin. Phys. B* **24** 060508
[9] Xin B and Zhang J 2015 *Nonlinear Dyn.* **79** 1399
[10] Cafagna D and Grassi G 2015 *Chin. Phys. B* **24** 080502
[11] Jia H Y, Chen Z Q and Qi G Y 2011 *Nonlinear Dyn.* **65** 131
[12] Zambrano-Serrano E, Campos-Cantón E and Muñoz-Pacheco J M 2016 *Nonlinear Dyn.* **83** 1629
[13] Jia H Y, Chen Z Q and Qi G Y 2013 *Nonlinear Dyn.* **74** 203
[14] Dong E Z, Liang Z H, Du S Z and Chen Z Q 2016 *Nonlinear Dyn.* **83** 623
[15] Wang Q X, Yu S M, Guyeux C, Bahi J and Fang X L 2015 *Chin. Phys. B* **24** 060503
[16] Zhou Y, Ionescu C and Machado J A T 2015 *Nonlinear Dyn.* **80** 1661
[17] Rajagopal K, Karthikeyan A and Srinivasan AK 2017 *Nonlinear Dyn.* **87** 2281
[18] Dong E Z, Chen Z P, Chen Z Q and Yuan Z Z 2009 *Chin. Phys. B* **18** 2680
[19] Luo C and Wang X 2013 *Nonlinear Dyn.* **71** 241
[20] Ahmad W M and Sprott J C 2003 *Chaos Soliton. Fract.* **16** 339
[21] Lu J G and Chen G R 2006 *Chaos Soliton. Fract.* **27** 685
[22] Lu J G 2006 *Phys. Lett. A* **354** 305
[23] Gao Z and Liao X 2012 *Nonlinear Dyn.* **67** 1387
[24] Li C G and Chen G R 2004 *Phys. A* **341** 55
[25] Ahmad W M and Sprott J C 2003 *Chaos Soliton. Fract.* **16** 339
[26] Smale S 1967 *Bull. Amer. Math. Soc.* **73** 747
[27] Kennedy J, Kocak S and Yorke J A 2001 *Am. Math. Mon.* **108** 411
[28] Kennedy J and Yorke J A 2001 *Trans. Amer. Math. Soc.* **353** 2513
[29] Yang X S, Yu Y G and Zhang S C 2003 *Chaos Soliton. Fract.* **18** 223
[30] Yang X S and Li Q D 2004 *Int. J. Bifurc. Chaos.* **14** 1847
[31] Yang X S and Li Q D 2006 *Chaos Soliton. Fract.* **27** 25
[32] Wiggins S 2003 *Introduction to Applied Nonlinear Dynamical Systems and Chaos* (New York: Springer)
[33] Fan Q J 2010 *Chin. Phys. B* **19** 120508
[34] Li Q D, Chen S and Zhou P 2011 *Chin. Phys. B* **20** 010502
[35] Guo Y and Qi G Y 2015 *J. Appl. Anal. Comput.* **5** 168
[36] Wang Z L, Zhou L L, Chen Z Q and Wang J Z 2016 *Nonlinear Dyn.* **83** 2055
[37] Xu Y M, Wang L D and Duan S K 2016 *Acta Phys. Sin.* **65** 120503 (in Chinese)
[38] Akgul A, Calgan H, Koyuncu I, Pehlivan I and Istanbullu A 2016 *Nonlinear Dyn.* **84** 481
[39] Alçın M, Pehlivan İ and Koyuncu İ 2016 *Optik Int. J. Light Electron Opt.* **127** 5500
[40] Ferdi Y 2009 *Comput. Electr. Eng.* **35** 722